UCRL - 76477
PREPRINT
Conf-750110--7

LAWRENCE LIVERMORE LABORATORY
University of California/Livermore, California

THE EFFECTS OF FLUID INSTABILITIES ON LASER FUSION PELLETS

W. C. Mead and J. D. Lindl

January, 1975

This paper was prepared for submission to the Orbis Scientiae II, January 19-24, 1975, University of Miami, Coral Gables, Florida and for publication in the proceedings.

THE EFFECTS OF FLUID INSTABILITIES ON LASER FUSION PELLETS

W. C. Mead and J. D. Lindl

January, 1975

This paper has been prepared for presentation at the Orbis Scientiae II, Jan. 19-24, 1975, University of Miami, Coral Gables, Florida and for publication in the proceedings.

Work performed under the auspices of the U.S. Atomic Energy Commission

I. INTRODUCTION

Recently a number of publications have dealt with the phenomena of Taylor instability in attempts to determine how the classical Taylor picture is modified in the presence of ablation and energy transport, and to estimate the importance of the effect to target implosion design. Stephen Bodner,[1] now at the Naval Research Laboratory, performed model calculations which indicated that ablative stabilization can partially eliminate Taylor growth.

Two different groups have performed instability analyses using one-dimensional linear perturbation codes to calculate growth rates. In these codes, the analytic equations governing fluid dynamics are transformed into a set of linearized equations governing the time evolution of perturbations, decoupled by an expansion in terms of spherical harmonics. These equations are then solved numerically with a combined zero-order/first order code to study the behavior of the instability. Shiau, Goldman, and Weng[2] at the University of Rochester, published results showing very high growth rates at long wavelengths and concluded that instabilities do grow in situations involving ablation. Henderson, McCrory, and Morse[3] at Los Alamos Scientific Laboratory, published results showing small or zero growth rates at long wavelengths and concluded that an ablation surface is positively stable.

In the present work, we have used an entirely different technique to study fluid instabilities, based upon direct two-dimensional simulation of the fluid flow and plasma physics. The

computer code LASNEX, written by G. Zimmerman[4] of Lawrence Livermore Laboratory, is a direct numerical solution of the two-dimensional fluid dynamics problem. The code models the plasma phenomena of laser light absorption by inverse bremsstrahlung and plasma instabilities; energy transport and partition, using flux-limited diffusion and separate ion, electron, and radiation temperatures; and, optionally, effects of multigroup photon and particle transport and magnetic field physics. The fluid dynamics itself is Lagrangian, with an equation of state used to determine pressure, energy, and opacity as a function of density and temperature. Thermonuclear burn of compressed matter is included to permit evaluation of output to input energy ratios.

The fluid instabilities are studied by applying a perturbation to a spherical shell or solid drop, then observing the amplitude of the disturbance as a function of time and position as the acceleration or implosion takes place. In the discussion to follow, unless otherwise specified, all LASNEX perturbation amplitudes will be RMS deviations of the Lagrangian quantities from average values along a symmetry direction, e.g.,

$$ZRMS_L = \left[\frac{\sum_{K=1}^{KMAX} (Z_{K,L} - \bar{Z}_L)^2}{KMAX} \right]^{1/2}$$

is the perturbed z-coordinate. This quantity may be plotted at a given time as a function of space or as a function of time for either a constant material point or for matter at a fixed position relative to the ablation front.

In the following, we shall discuss code tests and anomalies, comparison with previous work, our current understanding of fluid instability in the presence of ablation, and the implications of these results for laser fusion target design.

II. CODE TESTS

Consider now test cases consisting of slabs accelerated by a pressure source. Such problems can readily be calculated by LASNEX using an ideal gas equation of state. By using a large Γ, the material becomes essentially incompressible. If the material's temperature is large enough, the sound speed allows communication over distances of order of a wavelength in times short compared to the growth time for perturbations. That is, for incompressibility to hold, these problems satisfy $kc_s/\gamma \gg 1$, and are free of shock effects. The results for twenty problems with Atwood number 1.0, having a wide range of parameters, show that the ratio of growth rate computed by LASNEX to that computed from classical Taylor instability theory is .9 ± .2, as indicated in Figure 1.

The next two illustrations show the result of acceleration of compound slabs having an interface with Atwood number equal to ± .5. Figure 2 shows a comparison of the Atwood number + .5 interface LASNEX amplitude vs time with that of Taylor incompressible theory. The LASNEX growth rate is 23% low, and clearly shows reduced growth from the unstable Atwood number 1.0 interface. Figure 3 shows the amplitudes vs time for the same slab with the acceleration reversed. In this example, the Atwood number - .5 interface is correctly shown to be stable by LASNEX, exhibiting only a weak oscillation in perturbation phase, with no growth in magnitude.

Another test class of problems is the spherical shell driven by an external pressure source. An analytic solution for this geometry was presented by M. S. Plesset[5] for an Atwood number 1.0 spherical interface. The results of twelve test cases show the average ratio of LASNEX to analytic growth rates to be .8 ± .2.

The various non-ablating test problems have been examined to determine the severity of some sources of systematic error in the growth rates. The effect of primary concern is the growth rate reduction of about 20% caused by zoning the waveform as a ramp with 4 zones per wavelength. This perturbation form has been used frequently in problems with LASNEX, since the waveform is quite stable, allowing single wavelength studies to be made without growth of shorter wavelengths, which are damped by the code's artificial viscosity. Calculations begun with more than 4 zones per wavelength initially show improved agreement with classical theory, but eventually shift to shorter wavelengths which emerge as a result of noise in the impressed waveform and the higher growth rates for short wavelengths. The remaining zoning modifications tested were found to be insignificant for the intended uses of the code.

III. FLUID INSTABILITY AT AN ABLATING INTERFACE

We now turn to consideration of cases with ablation. Here theory becomes extremely difficult and the theoretical results available have limited application to the problems of interest.

Our early applications of LASNEX to laser pellet implosions gave little evidence of ablative stabilization of Taylor growth, so a comparison of considerable interest was to apply LASNEX to the solid drop, apparently stable implosion published by Henderson, et al.,[3] of Los Alamos Scientific Laboratory (LASL).

The case they considered was a 500 μm radius DT sphere of initial density .21 g/cm^3, irradiated by a laser of 1.06 μm wavelength. The laser energy was 50 KJ in a Gaussian pulse of 550 psec full width at half maximum. The zero order solution was calculated in a 1 temperature Lagrangian hydrodynamics code with electron thermal conduction. In order to reproduce the LASL zero order solution for this implosion, LASNEX was run with artificially high electron-ion coupling, with all flux limiters turned off, and with no radiation physics. The resulting LASNEX calculation, shown in Figure 4, agrees fairly well with the published results of LASL, shown for comparison purposes. Plotted here are the density vs radius profiles at t = + .24 ns and t = + .53 ns with respect to the peak of the Gaussian pulse and the temperature profile at t = + .24 ns.

The first order perturbed quantities are presented by LASL only for the relatively long wavelength modes ℓ = 2, 3 and 5. The modes ℓ = 2 and 5 were run with LASNEX. The pellet surface was

initially perturbed with a spherical harmonic of amplitude .5μm RMS. In Figure 5 are shown the $\ell = 5$ perturbed density vs position and the perturbed temperature vs position at the same implosion times as the zeroth order profiles. Agreement between the two codes is qualitatively good, and quantitative within an overall factor of three in amplitude.

We also ran the $\ell = 100$ mode with LASNEX, for which the classical Taylor prediction for the number of e-foldings is about 8.9, corresponding to a growth factor of about 10^4 in amplitude. The results of this run indicate definite suppression of Taylor growth and thus a significant stabilization of the interface.

The implosion of this pellet raises interesting questions about stabilization which were addressed by a series of test problems. Using a 450 μm radius bare DT drop and a 60 kJ laser pulse of 1.06 μm wavelength, a partially optimized 1-D implosion was designed which, according to LASNEX's default physics, achieved a thermonuclear energy yield of 550 kJ. The pulse for this implosion had the time profile shown in Figure 6a. A series of 2-D LASNEX calculations was then made, progressing from a highly chopped pulse, which included only the high energy tail, towards the fully optimized pulse. The most severly chopped pulse (A) produces an implosion which has a basic similarity to the previous case: the density of compressed matter is essentially constant during the implosion, while its temperature continually rises.

This is evident in Figure 6b, which shows the material adiabats for the various pulses. As the pulse is extended to lower initial power levels, the material achieves increasingly isentropic compressions, moving towards the optimized case which achieves a peak density of 300 and a ρr of 1.2 g/cm^2.

The plot of Figure 6c shows the 1-D yield ratio and the number of e-foldings observed in the LASNEX calculated perturbed spherical radius as a function of pulse start-time for the ℓ = 100 mode. The most extreme shortened pulse shows characteristics very similar to the LASL case. As the pulse is extended, the instability begins to grow, until, for the optimized case, the amplitudes exhibit enough growth to make the implosion calculation fail before completion. It is evident that the thermonuclear yield is reduced significantly before any significant instability growth rate reduction is achieved.

This example and others point out the general characteristics of the only known class of strongly stabilized ablative accelerations. The stable situation occurs under these conditions:

1. accelerated matter forms a more or less constant density shell
2. the shell is propagating as a shock of increasing strength through cold matter, hence the material in the shocked-up shell has a continually worsening adiabat
3. ablation rate is nearly equal to the rate of mass intake at the front of the shock
4. thermal conduction times across the shocked shell

are short enough to readily transmit thermal energy to the shock front.

In light of condition 2, it appears that the stabilization evidenced may be difficult to apply to a target implosion having significant thermonuclear yield.

IV. EFFECTS OF FLUID INSTABILITY ON LASER FUSION TARGETS

Next, consider the implications of these findings for laser-fusion targets. We consider here shells of pure DT with aspect ratios ($r/\Delta r$) varying from 60:1 to 1:1 where r is the radius and Δr is the thickness of the shell. We limit present discussion to laser energy in the 100 kJ range and to targets which give a yield ratio (fusion energy out/laser energy in) in the range 20 to 60.

Interest in the use of hollow shells stems from the fact that they can be imploded using a lower laser power and less severe pulse shaping. This arises from the fact that one must do a certain minimum of work on the DT fuel to compress and ignite it. This work is $W = \int PdV$ where P is the applied pressure and V is the volume. By increasing the volume, you decrease the required pressure and laser power. Lower power is important for two reasons:

a) Lower power means lower cost for the laser.

b) The existence of parametric plasma instabilities and resonance absorption processes lead to the production of very energetic electrons when a threshold laser intensity is reached. These energetic electrons result in preheat of the fuel and a drop in the driving pressure because of decoupling.

In most cases of interest to laser fusion, the Atwood number is about one so that for classical Rayleigh-Taylor instability we have $\gamma \sim \sqrt{ka}$, k is the wavenumber of the perturbation and a is the acceleration. Three ranges of wavelengths and physical effects are important.

a) $\lambda >> \Delta x_{min}$ where Δx_{min} is the minimum shell thickness: The effect of perturbations at these wavelengths is to reduce the overall symmetry of the implosion. With convergence ratios, given by the ratio of the initial radius to the final radius, on the order of 100, the symmetry and uniformity of implosion velocities must be maintained within a percent or so in order to get good spherical convergence and conversion of kinetic energy to thermal energy at the end of the implosion. Since long wavelengths have small growth rates, they generally do not cause a problem if the effects of shorter wavelengths can be tolerated.

b) $\lambda \sim \Delta x_{min}$: Wavelengths of this size result in a breakup of the shell and a gross mixing of high and low density matter. Perturbations of this size have high growth rates compared to the wavelengths which affect the overall symmetry and require much smaller surface perturbations. They are consequently much more difficult to live with.

c) $\lambda << \Delta x_{min}$: Short enough wavelengths are stabilized by viscosity and density gradient effects. But there is a range of wavelengths which have even higher growth rates than those for $\lambda \sim \Delta x_{min}$. These wavelengths reach the non-linear bubble and spike phase with an amplitude about equal to a wavelength and only grow linearly in time beyond this point. Perturbations at these wavelengths

do not become as large as the shell thickness before being overtaken by perturbations at longer wavelengths which are still growing exponentially. The primary effect of these wavelengths is expected to be a modification of matter and energy transport at the ablation surface. We are not able to study this effect directly with Lasnex because a Lagrangian code cannot handle the non-linear turbulent stage of evolution.

We deal at present with the wavelength range (b), and with the picture of fluid instability for which LASNEX predicted growth rates are in the range of 50 - 100% of classical Taylor values.

In general, there are two sources for perturbations that can be amplified by Rayleigh Taylor instability: 1) surface perturbations due to imperfections during the manufacturing process; and 2) laser irradiation non-uniformity. Non-uniform illumination is essentially equivalent to a surface perturbation because the difference in intensity across the surface results in the imprinting of a surface perturbation. After the initial imprinting has occured, the exponential growth due to the Rayleigh-Taylor instability quickly dominates the effect of a non-uniform intensity. Use of a preheated, low density atmosphere can greatly reduce the effects of such a laser perturbation, because lateral heat conduction will smooth out the variation.

Consider a 30-1 shell whose initial radius was 1.5 mm, which had an atmosphere density of 3×10^{-4} gm/cc extending to 4.2 mm,

preheated to 1 keV by a 7.5 kilojoule (kJ) prepulse of 4 μ light, as shown in Figure 7. A 4.5° per wavelength variation in intensity (ℓ = 80) was equivalent to .0043 Å surface perturbation per percent variation when magnetic fields are not induced. When the production of magnetic fields by the non-uniform laser is included, and the transport co-efficients of Braginskii are used, the laser intensity variation is equivalent to .15 Å per percent at the same wavelength. For longer wavelengths, lateral heat conduction is not as effective at smoothing the intensity variation. However the growth rate is smaller so there is a tradeoff which varies from case to case and depends on the temperature, density distribution and radius of the atmosphere. Because the effects of non-uniform illumination depend on many parameters which are not relevant to Rayleigh-Taylor instability, we have concentrated most of our effort on targets with a given initial surface perturbation and uniform illumination.

To optimize an implosion to survive shell break-up from fluid instabilities (in the absence of strong ablative stabilization), the essential criteria are:

1) minimize the final velocity: to some extent a trade-off can be made between final velocity and peak laser power, within the constraint of satisfying pellet ignition conditions;
2) maximize the average acceleration: for a given final velocity, the earlier and larger the acceleration, the fewer instability e-foldings will result, but the

maximum acceleration abtainable is limited by requirements for an isentropic compression;

3) maximize the minimum shell thickness: since longer wavelengths grow more slowly, considerable reduction in growth can be achieved by keeping the shell thickness as large as possible, particularly during the late parts of an implosion.

Figure 8 shows the characteristics of the implosion of a 30:1 shell optimized according to these criteria. The pulse shape is shown in Figure 8a and the velocity history in Figure 8b. Amplitudes for various perturbation modes are shown as solid curves in Figure 8c. The dashed curve shows the shell thickness history. With its outer surface perturbed by an initial amplitude of 7 Å RMS, the shell could not be successfully imploded at modes higher than $\ell = 160$. The growth rate increases more slowly than the $\sqrt{\ell}$ scaling to be expected from the classical incompressible solution. For $\ell = 80$, the growth rate shown is 80% of the Plessett prediction, while for $\ell = 640$, the rate is 50% of the Plessett value. The plot of Figure 8d shows isodensity contours at the time of break-up of this 30:1 shell, for an $\ell = 320$ mode. When the shell has disintegrated to this extent, no significant thermonuclear yield can be obtained.

Figure 9 indicates the ratio of the number of e-foldings expected at the worst wavelength to the maximum tolerable number of e-foldings as a function of $r/\Delta r$. This ratio is estimated by taking the square root of the ratio of the worst wavenumber to the largest wavenumber at which success was achieved. The maximum tolerable number of e-foldings is calculated on the basis of a 10 Å initial perturbation. Each of the numbers indicated is the best case at that $r/\Delta r$, which in each case was achieved with the most rapid acceleration possible, consistent with high gain. The last entry, for a 2 1/3 - 1 shell is for a continuously accelerated shell that successfully imploded with a 1 Å surface finish at the worst wavelength.

Instead of applying a continuous power source, one can impulsively accelerate the target by turning the laser on and off. In this way, the target is subjected to bursts of very rapid acceleration followed by near coasting. After the passage of each impulse, the perturbations do not grow exponentially but they do grow linearly. As given by Richtmeyer,[6]

$$\dot{a} = k\Delta v \alpha a_0$$

where Δv is the velocity of the material behind the shock relative to that in front of the shock, a_0 is the initial amplitude, α is the Atwood number and $\dot{a}$ is the time rate of change of the amplitude. This growth arises because of shock focusing as the shock passes a perturbed surface. The smallest growth possible occurs when the shell receives its entire velocity from a single shock. In this case, the growth

factor is given approximately by

$$\frac{a}{a_0} = kR.$$

This growth factor is a lower limit to what one can achieve with implosions subject to Rayleigh-Taylor instability. For the 2 1/3 - 1 shell considered below, this factor is 160 or 5 e-foldings. With such growth, one could tolerate an initial perturbation of a couple hundred angstroms. However, the growth factor increases as more shocks are used, and several shocks are necessary to maintain near adiabatic compression. In the limit of a large number of weak shocks, the growth factor goes over to the Rayleigh-Taylor value.

By suitably timing the several pulses and keeping the ratio of magnitudes of succeeding shocks within a factor of 2-3, one can decrease the number of generations and maintain isentropic compression and high gain. Using this technique, we are able to lower the power to 10^{14} watts, an order of magnitude lower than for a typical solid sphere and survive with a 15 Å surface finish. The pulse shape and velocity history for this implosion are shown in Figures 10a and 10b. Perturbation amplitude and shell thickness versus time are shown in Figure 10c. The peak laser intensity is about 2×10^{15} w/cm^2 at a peak temperature of 5 keV. This intensity is about an order of magnitude above the calculated threshold for the parametric decay instability at 1/4 μ, although about 85% of the light is absorbed by inverse Bremsstrahlung.

We expect to be able to live with this intensity by seeding with a higher Z material. Improvements in the impulsive acceleration technique may allow us to further lower the intensity.

V. CONCLUSIONS

Our tests of LASNEX indicate that the code can be successfully used to study fluid instability. We expect final amplitudes to be accurate to within a factor of 3 or 20% in e-foldings, whichever is larger, on the basis of known systematic errors.

We find that suppression of fluid instability growth does occur for a class of highly non-adiabatic implosions, but that the effect is not significant for isentropic implosions of primary interest for laser fusion.

For isentropic compressions, LASNEX predicts growth rates for wavelengths on the order of the shell thickness in the range of 50 - 100% of classical Taylor/Plessett values, with systematic reduction in the ratio of LASNEX to classical growth rates at shorter wavelengths. With this instability behavior, the parameter space for successful laser fusion target design is restricted to some extent.

Our calculations show, however, that even in this quite pessimistic view of instability growth, shells of low aspect ratio can be imploded isentropically. Particularly, if impulsive acceleration is used during the early part of the implosion, an initial surface perturbation of a few tens of angstroms can be tolerated at the worst shell break-up wavelengths. It looks possible to achieve these surface finishes. Further, it should be possible to produce an atmosphere around the pellet which will reduce the imprint from non-uniform illumination to tolerable levels.

ACKNOWLEDGEMENT

The authors would like to express their appreciation for many helpful discussions with John Nuckolls. Many thanks are due George Zimmerman for cooperating with our use of LASNEX.

REFERENCES

1. S. Bodner, Phys. Rev. Lett. 33, 761 (1974).

2. J. N. Shiau, E. B. Goldman, and C. I. Weng, Phys. Rev. Lett. 32, 352 (1974).

3. D. B. Henderson, R. L. McCrory, and R. L. Morse, Phys. Rev. Lett. 33, 205 (1974)

4. G. B. Zimmerman, Univ. of Calif. Report UCRL-74811 (1973).

5. M. S. Plesset, J. of Appl. Phys. 25, 96 (1954).

6. R. D. Richtmeyer, Comm. on Pure and Appl. Math, XIII, 297-319 (1960).

FIGURE CAPTIONS

Figure 1: Summary of LASNEX code tests in plane and spherical geometry.

Figure 2: Amplitude (ZRMS) vs time for slab accelerations (unstable). The compound slab consisted of two .02 cm thick DT regions of density .105 g/cm^3 and .21 g/cm^3, yielding an Atwood number of .5 at the common interface. A pressure source of 50. Mb was applied to the free boundary of the low density region. The amplitude vs time is shown for all three interfaces in the test problem, together with the amplitude predicted by incompressible Rayleigh-Taylor theory. The perturbation wavelength was .036 cm.

Figure 3: Amplitude (ZRMS) vs time for slab acceleration (stable). This problem had the same parameters as that of Figure 1, but the pressure source was applied to the high density free boundary. The acceleration was thus in the stable direction for the Atwood number -.5 interface.

Figure 4: Zero order density and temperature profiles. For a DT sphere having initial density .21 g/cm^3 and radius of .05 cm, irradiated by a 1.06 μm laser pulse with a Gaussian time profile (FWHM = 550 psec), this figure shows sample snapshots of density and temperature. The solid curves show LASNEX results with parameters adjusted to simulate the results of Henderson, McCrory and Morse. The two comparison times are + .24 ns and + .53 ns with respect to the time of peak laser power.

Figure 5: First order perturbed density and temperature profiles. For the same case as Figure 3, this figure presents snapshots of perturbed densities and temperature at corresponding times. The LASNEX results, shown as the solid curve, are RMS amplitudes for an $\ell = 5$ perturbation of initial RMS amplitude .5 μm. The profiles published by Henderson, McCrory and Morse are shown for comparison. Note that the time evolution and density profiles are very similar, but a factor of 2 discrepancy in initial amplitude does not show in the figure, since the calculation of Henderson, et al., was done with 1. μm initial amplitude.

Figure 6a: Pulse shapes for stability example. The solid curve shows the semi-optimized time profile of a 60 kJ, 1.06 μm laser pulse for a .045 cm radius DT sphere. The pulse (D) yields peak density of 300 g/cm^3 and about 550 kJ of thermonuclear energy in a 3-temperature, 1-D model. The time intervals indicated by A,B and C show truncations used in studying stabilization of the implosion. Pulse shape A gives stability comparable to the 50 kJ, 550 ps FWHM gaussian, shown as a dashed line.

6b: Implosion adiabats.

6c: 1-D energy yield ratios and 2-D calculated e-foldings.

Figure 7: Effects of Non-Uniform Illumination. The 30:1 shell shown here has a pre-pulse heated atmosphere. Laser illumination non-uniformity imprints an initial effective surface perturbation which subsequently grows with the same rate as a surface perturbation with uniform illumination.

Figure 8: 30:1 shell a) Laser pulse shape. b) Velocity history. The shell for this calculation had no atmosphere and was uniformly illuminated. The initial radius was .15 cm c) Amplitude and shell thickness history. The "shell thickness" is the distance separating the two points at which density is 30% of the maximum density. d) Iso-density plot. The mode ℓ = 320 fails at time 4.3 nsec, well before the shell reaches the origin.

Figure 9: Estimated $n_{LASNEX}/n_{TOLERABLE}$ vs aspect ratio. The ratio of LASNEX calculated e-foldings (n_{LASNEX}) to the tolerable number ($n_{TOLERABLE}$), assuming an initial 10 Å surface perturbation improves as the aspect ratio ($r/\Delta r$) decreases. These results are scaled from 2-D calculations of optimized implosions at the indicatd aspect ratio.

Figure 10: 2:1 shell a) Laser pulse shape. b) Velocity history. The shell for this calculation initially extended from .04 cm to .07 cm at a density of .21 g/cc. The impulsive acceleration helps reduce fluid instability growth. c) Amplitude and shell thickness histories. Calculations show that this shell could be successfully imploded at any wavelength with an initial amplitude of 15 Å or greater.

Slab geometry 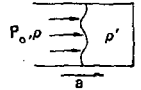 	Classical Taylor $\eta = \eta_o e^{\gamma t}$ Amplitude $\gamma = \sqrt{\alpha k a}$ Growth rate $\alpha = (\rho' - \rho)/(\rho' + \rho)$ Atwood number	LASNEX results, $\alpha = 1$ 20 cases, $\frac{\gamma_{ASNEX}}{\gamma_{Taylor}} = .9 \pm .2$ $\frac{kc_s}{\gamma} >> 1$ $k\eta < 1, kd >> 1$
Spherical geometry  	Plessett solution J. Appl. Phys. 25, 96 (1954)	LASNEX results 12 cases, $\frac{\gamma_{LASNEX}}{\gamma_{Plessett}} = .8 \pm .2$

FIGURE

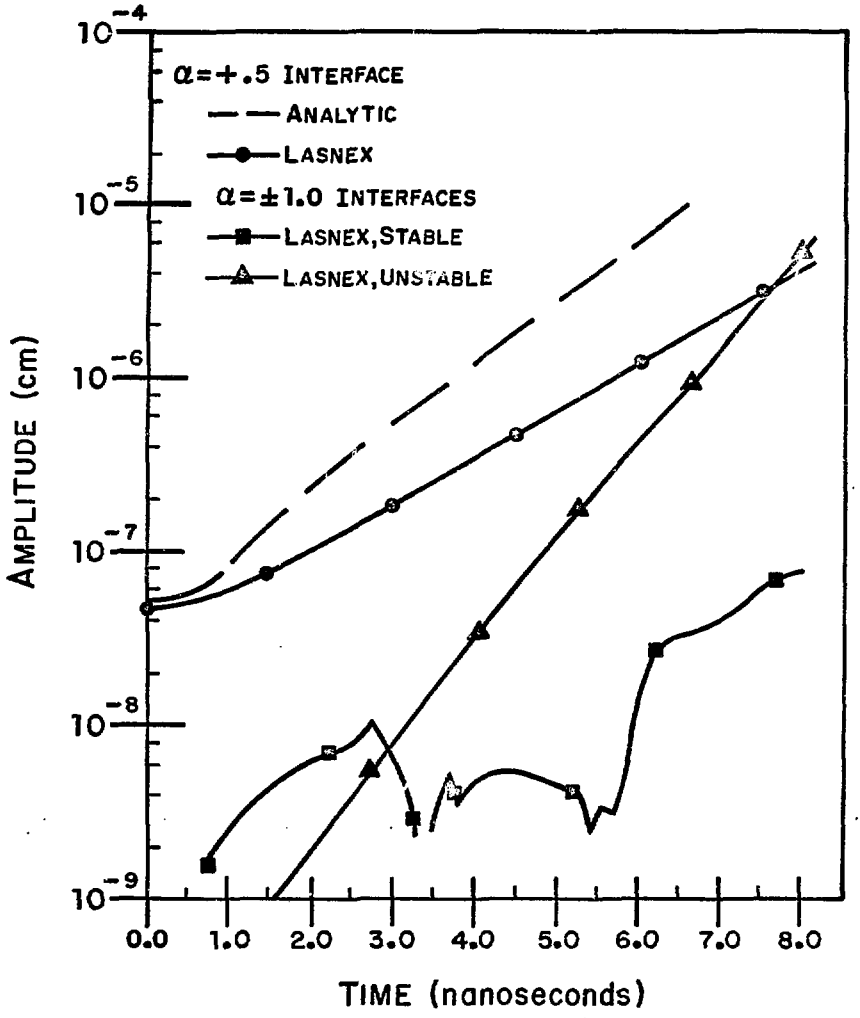
α=+.5 INTERFACE
ANALYTIC
LASNEX
α=±1.0 INTERFACES
LASNEX,STABLE
LASNEX,UNSTABLE
AMPLITUDE (cm)
10^-4
10^-5
10^-6
10^-7
10^-8
10^-9
0.0
1.0
2.0
3.0
4.0
5.0
6.0
7.0
8.0
TIME (nanoseconds)

FIGURE 2

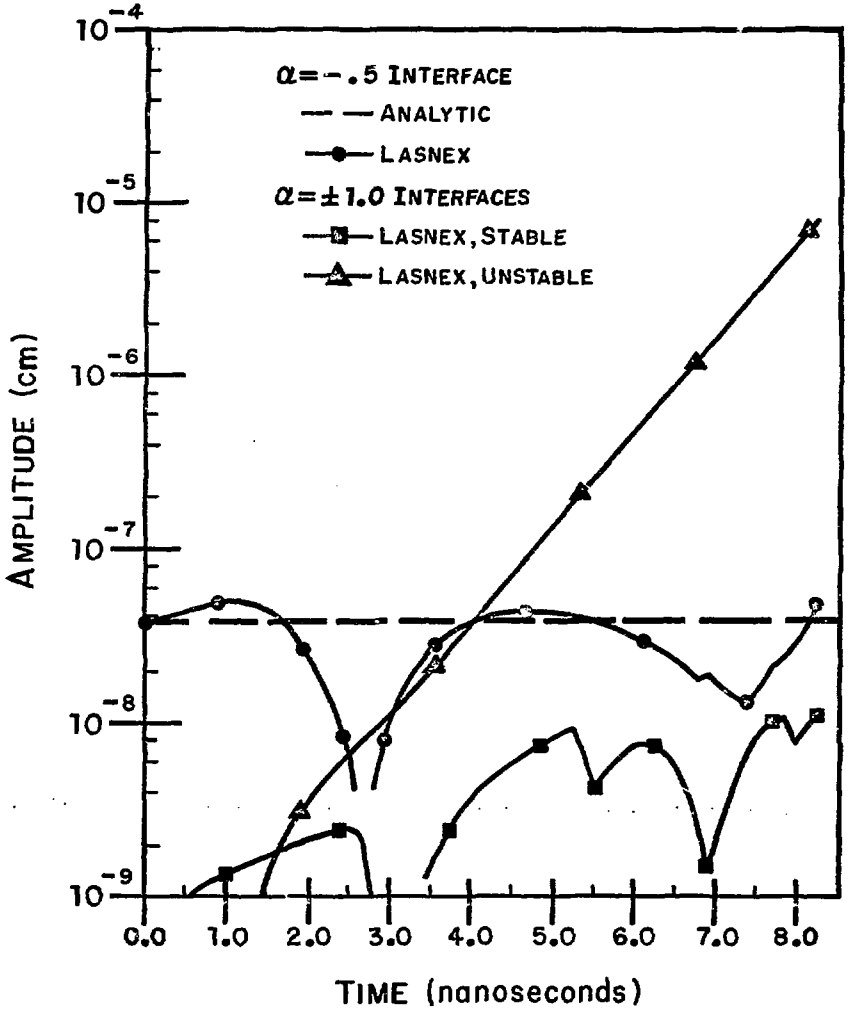
α = −.5 INTERFACE
ANALYTIC
LASNEX
α = ±1.0 INTERFACES
LASNEX, STABLE
LASNEX, UNSTABLE
AMPLITUDE (cm)
10^-4
10^-5
10^-6
10^-7
10^-8
10^-9
0.0
1.0
2.0
3.0
4.0
5.0
6.0
7.0
8.0
TIME (nanoseconds)

FIGURE 3

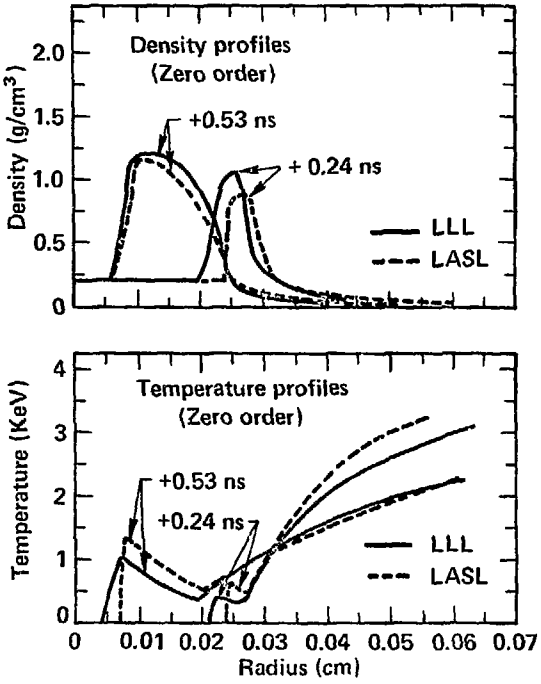
Density profiles
(Zero order)
Density (g/cm³)
2.0
1.5
1.0
0.5
0
+0.53 ns
+ 0.24 ns
LLL
LASL
Temperature profiles
(Zero order)
Temperature (KeV)
4
3
2
1
0
+0.53 ns
+0.24 ns
LLL
LASL
0
0.01
0.02
0.03
0.04
0.05
0.06
0.07
Radius (cm)

FIGURE 4

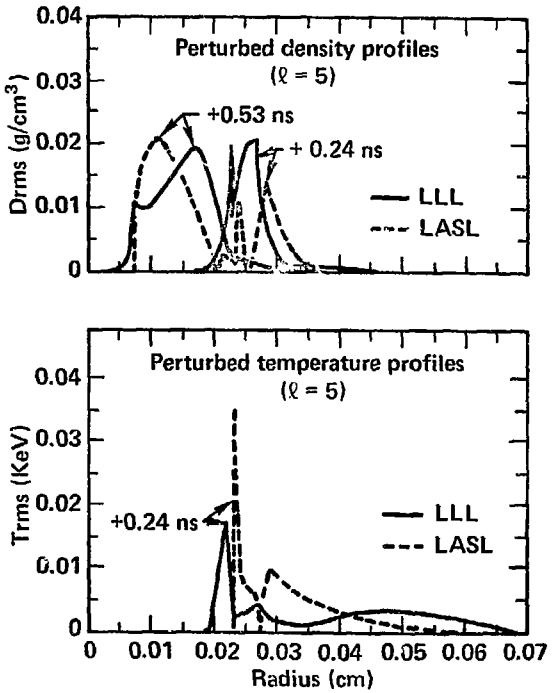
Perturbed density profiles
(ℓ = 5)
+0.53 ns
+ 0.24 ns
LLL
LASL
Drms (g/cm³)
0.04
0.03
0.02
0.01
0
Perturbed temperature profiles
(ℓ = 5)
+0.24 ns
LLL
LASL
Trms (KeV)
0.04
0.03
0.02
0.01
0
0 0.01 0.02 0.03 0.04 0.05 0.06 0.07
Radius (cm)

FIGURE 5

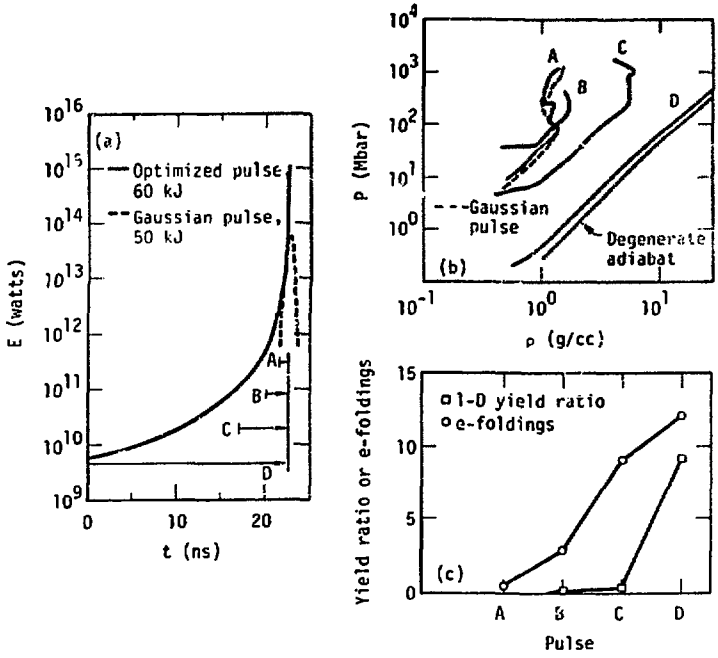
(a)
Optimized pulse, 60 kJ
Gaussian pulse, 50 kJ
E (watts)
t (ns)
A
B
C
D
(b)
Gaussian pulse
Degenerate adiabat
ρ (Mbar)
ρ (g/cc)
(c)
1-D yield ratio
e-foldings
Yield ratio or e-foldings
Pulse

FIGURE 6

Illuminated with a 4 μ laser

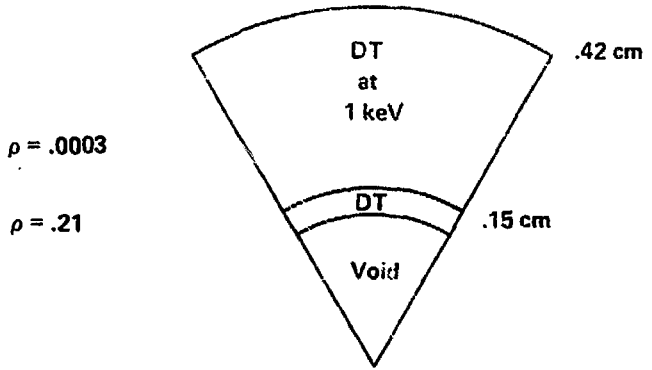

No magnetic field generation	.0043 Å per percent
With magnetic field generation using transport coefficients of Braginskii	.15 Å per percent

FIGURE 7

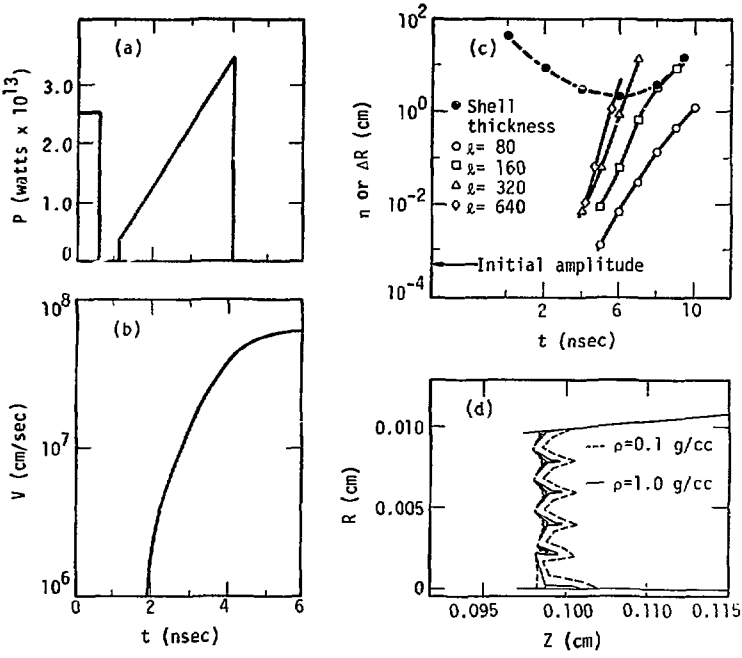
(a)
P (watts x 10^{13})
3.0
2.0
1.0
0
(b)
V (cm/sec)
10^8
10^7
10^6
0
2
4
6
t (nsec)
(c)
n or ΔR (cm)
10^2
10^0
10^{-2}
10^{-4}
Shell thickness
ℓ= 80
ℓ= 160
ℓ= 320
ℓ= 640
Initial amplitude
2
6
10
t (nsec)
(d)
R (cm)
0.010
0.005
0
--- ρ=0.1 g/cc
— ρ=1.0 g/cc
0.095
0.100
0.110
0.115
Z (cm)

FIGURE 8

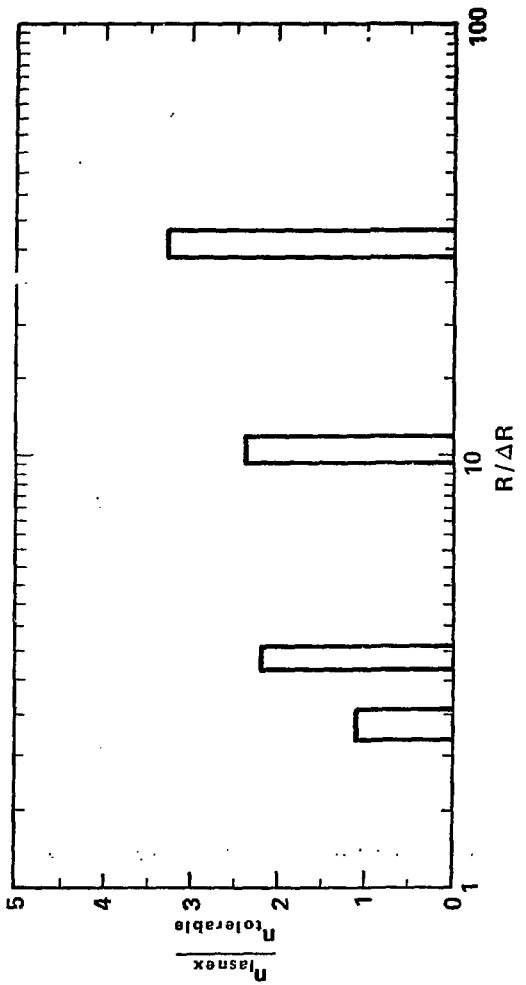

FIGURE 9

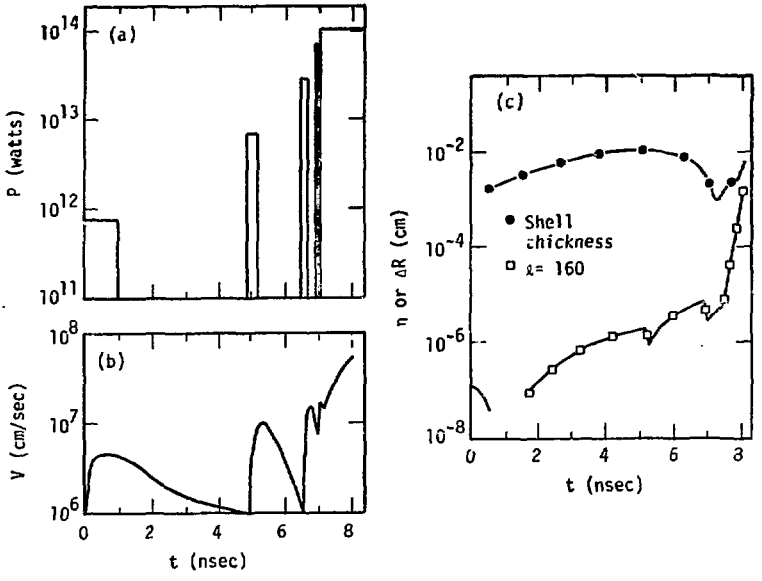
(a)
P (watts)
10^{14}
10^{13}
10^{12}
10^{11}
(b)
V (cm/sec)
10^{8}
10^{7}
10^{6}
0
2
4
6
8
t (nsec)
(c)
η or ΔR (cm)
10^{-2}
10^{-4}
10^{-6}
10^{-8}
● Shell thickness
□ ℓ= 160
0
2
4
6
8
t (nsec)

FIGURE 10